

Giant Linear Dichroism Controlled by Magnetic Field in FePS₃

Xu-Guang Zhou,^{1,*} Zhuo Yang,^{1,*} Youjin Lee,^{2,3} Jaena Park,^{2,3} Yoshimitsu Kohama,¹ Koichi Kindo,¹ Yasuhiro H. Matsuda,¹ Je-Geun Park,^{2,3} Oleg Janson,^{4,†} and Atsuhiko Miyata^{1,‡}

¹*Institute for Solid State Physics, University of Tokyo, Kashiwa, Chiba 277-8581, Japan*

²*Center for Quantum Materials, Seoul National University, Seoul 08826, Republic of Korea*

³*Department of Physics and Astronomy, Institute of Applied Physics,*

Seoul National University, Seoul 08826, Republic of Korea

⁴*Institute for Theoretical Solid State Physics, Leibniz IFW Dresden, 01069 Dresden, Germany*

Magnetic-field control of fundamental optical properties is a crucial challenge in the engineering of multifunctional microdevices. Van der Waals (vdW) magnets retaining a magnetic order even in atomically thin layers, offer a promising platform for hosting exotic magneto-optical functionalities owing to their strong spin-charge coupling. Here, we demonstrate that a giant optical anisotropy can be controlled by magnetic fields in the vdW magnet FePS₃. The giant linear dichroism ($\sim 11\%$), observed below $T_N \sim 120$ K, is nearly fully suppressed in a wide energy range from 1.6 to 2.0 eV, following the collapse of the zigzag magnetic order above 40 T. This remarkable phenomenon can be explained as a result of symmetry changes due to the spin order, enabling minority electrons of Fe²⁺ to hop in a honeycomb lattice. The modification of spin-order symmetry by external fields provides a novel route for controllable anisotropic optical micro-devices.

Optical anisotropy constitutes a fundamental and crucial concept for linear and nonlinear optical components such as polarizers, wave plates, and phase-matching elements. It is a powerful tool not only for providing direct information on symmetry breaking but also as a key link in describing the quantum state of photons within the quantum mechanics framework [1]. To generate linearly polarized light, unpolarized light typically passes through a crystal with structural or electronic anisotropy. These anisotropies are achieved by using materials such as liquid crystals, polymers, and some birefringent crystals [2, 3]. While conventional materials providing linear polarizations have been successfully commercialized for many applications, their linear dichroism (LD) remains constant and uncontrollable. In particular, their intrinsic three-dimensional structure prevents its incorporation into micro-devices. Recent studies of two-dimensional materials with large LD effects provide a completely new path for the realization of micro-devices, such as the black phosphorus (BP) [4] and rhenium disulfide (ReS₂) [5]. Despite the excellent potential for application, reports on microdevices capable of controlling optical anisotropy remain scarce [6].

In contrast to traditional three-dimensional magnetic materials, van der Waals (vdW) magnets, which have been intensively studied recently, have a huge potential for developing micro-controllable optical devices. Like graphite, these materials can be exfoliated into a single layer, exhibiting fascinating mesoscopic properties, and maintaining bulk-like magnetic and multiferroic behavior even in a single monolayer [7, 8]. This makes them

easily stackable and allows for fabrication of functional heterostructures for micro-controllable devices. Remarkably, in vdW magnets, e.g., MPX_3 family, where M is a 3d transition element and X is S or Se [7], strong couplings between magnetism and electronic properties have been recently reported, leading to exotic optical properties such as coherent many-body excitons in NiPS₃ and giant linear dichroism in FePS₃ [9, 10]. In addition, external magnetic fields can play a crucial role in modifying such strong couplings and give rise to the emergence of novel magneto-optical properties in vdW magnets.

FePS₃ has a monoclinic structure with $C2/m$ symmetry. Below $T_N \sim 120$ K, it features an Ising-type zigzag order with magnetic chains running along the a axis [11–14]. Previous studies have revealed a giant LD effect near the band-gap energy (~ 1.4 -1.5 eV [12]) in this compound only below T_N [6, 10, 12], indicating that the magnetic order is crucial for the LD effect. Interestingly, using micro-nano fabrication techniques, a cavity-coupled FePS₃ exhibits the giant LD reaching up to almost 100% [6]. Furthermore, recent high-field magnetization experiments under an out-of-plane field revealed a sudden jump in magnetization at 40 T [15]. This is understood as an Ising-like spin-flip transition in FePS₃, where the spin configurations change from a zigzag antiferromagnetic order to a spin-polarized phase. The step-like magnetization curve implies that an external field is a promising way to realize the switch-like control of the giant LD effect.

In this study, we measured the magnetic field dependence of the LD effect in FePS₃ with \mathbf{B} of up to 52 T ($\mathbf{B} \parallel c$ axis). The results demonstrate a sudden jump in LD at 40 T, coinciding with the breakdown of zigzag spin order symmetry. Our findings support the notion that spin order symmetry is the primary factor influencing the LD effect. Furthermore, following the substantial

* These authors contributed equally to this work.

† o.janson@ifw-dresden.de

‡ a-miyata@issp.u-tokyo.ac.jp

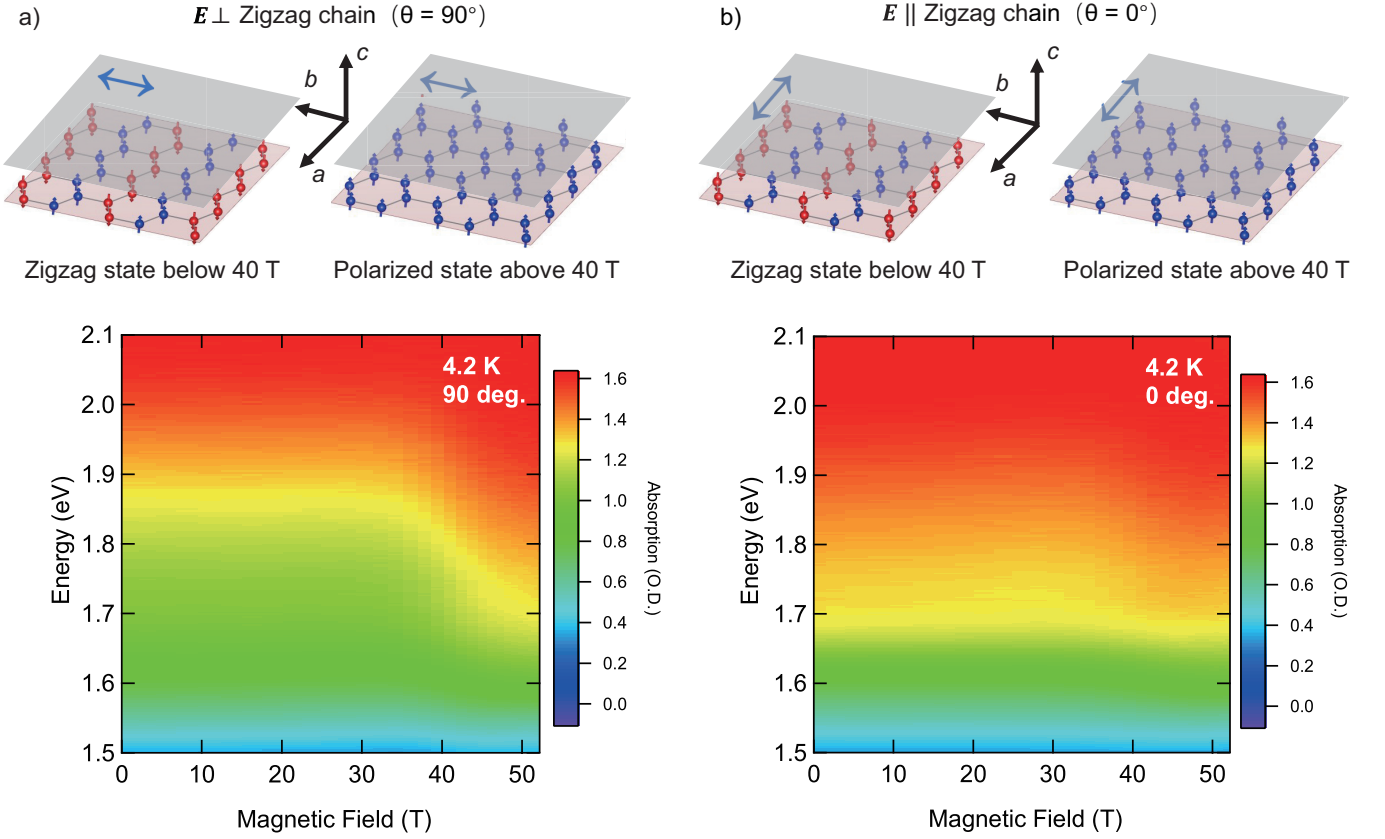


FIG. 1. The field-dependent absorption spectra of FePS₃ in two geometries, where zigzag chains are a) perpendicular and b) parallel to the \mathbf{E} polarization. The gray squares represent the neutral density linear polarizer, and the directions of \mathbf{E} is marked with the blue arrows. The spin order of an exfoliated multi-layered sample is drawn by the honeycomb lattice below the polarizer. The spectra are obtained at 4.2 K in helium gas environment and the external field is parallel to the c -axis.

jump in LD under an external field, we propose that a vdW antiferromagnet, FePS₃, can serve as a microdevice for the switch-like control of an optical anisotropy under a magnetic field. Given the precision and rapid regulation capabilities of external fields compared to temperature, such optical devices are anticipated to play an active role in quantum optics and optical computing. Note that cm-sized pulsed magnets are nowadays widely available.

FePS₃ flakes are mechanically exfoliated from a bulk crystal using Scotch tape and transferred onto the SiO₂ substrate. The size of SiO₂ substrate is 2 mm in diameter and 0.3 mm in thickness. The thickness of a FePS₃ sample is estimated to be 2-3 μm by the interference effect [16]. Magneto-absorption measurements are performed with a pulse magnet for magnetic fields up to 52 T. The pulse duration of the magnetic field is about 36 ms. The field direction and the propagation direction of light are along the c -axis of the FePS₃ sample (the Faraday configuration). The sample was mounted in a helium gas-filled tube which was placed in a liquid helium cryostat to achieve a low temperature of 4.2 K. A broad-band halogen lamp is employed as the light source. The

light emitted from the lamp is coupled to an 800 μm core diameter multimode fiber, used to illuminate the sample. The linear polarizer is placed between the excitation fiber and the sample, and the distance between the polarizer and the sample is less than 1 mm. The transmitted light is coupled in an 800 μm diameter multimode fiber and guided to a spectrometer equipped with a CCD camera. The typical exposure time of 0.5 ms is much shorter than the field duration, ensuring that the transmission spectra were acquired at essentially constant magnetic field values.

Figure 1 illustrates the field-dependent absorption spectra of FePS₃ in two distinct geometries, both acquired at 4.2 K. The absorption A is obtained by $-\log_{10} \frac{I}{I_0}$, where I is a transmitted intensity and I_0 an incident intensity. In the first geometry, as shown in Fig. 1(a), the zigzag chain (a axis) is perpendicular to the electric-field polarization of light \mathbf{E} , achieved using a neutral density linear polarizer. On the other hand, the second geometry, as shown in Fig. 1(b), presents the parallel condition. The angle between \mathbf{E} and the zigzag chain (a -axis) is denoted as θ . When θ equals 90°, the

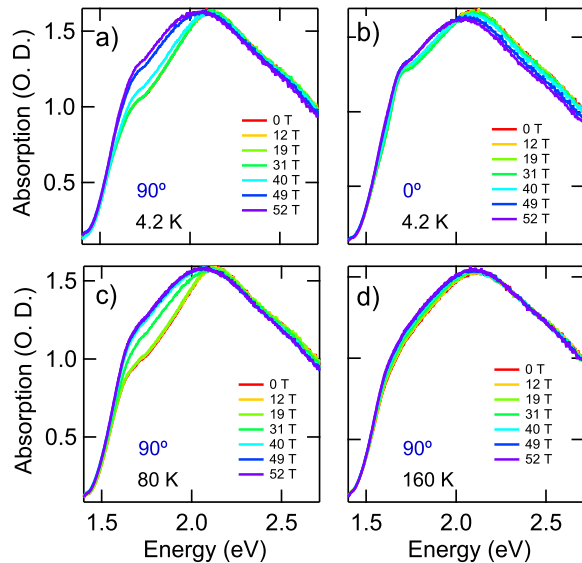


FIG. 2. Absorption spectra for different polarization angles and temperatures in magnetic field; a) 90° and 4.2 K, b) 0° and 4.2 K, c) 90° and 80 K, and d) 90° and 160 K. The change of absorption is only observed for $\theta = 90^\circ$ below T_N .

absorption spectra remain unchanged below an external field of 40 T. However, beyond this threshold, remarkably, the optical absorption in FePS_3 experiences a sudden enhancement around 1.7 eV. This behavior contrasts with the $\theta = 0^\circ$ case, as shown in Fig 1(b), where the absorption spectra are almost field-independent up to 52 T.

Differences between the two polarization angles become evident in 1D plots, where absorption is plotted as a function of energy by applying a magnetic field. In Fig. 2(a), i.e., $\theta = 90^\circ$, the optical absorptions between 1.6 eV and 2.0 eV are strongly suppressed without a magnetic field. This suppression remains almost intact up to the full magnetic polarization at 40 T, at which the absorption spectrum experiences a rapid enhancement before reaching saturation. Outside this energy range, no clear field dependence of the absorption spectrum is observed. In contrast, for $\theta = 0^\circ$, the optical absorption between 1.6 and 2.0 eV is not suppressed at 0 T (i.e., the observation of the giant LD effect). For $\theta = 0^\circ$, almost no magnetic field dependence is observed (Fig. 2, b).

In order to better understand the impact of spin order on the field-induced change of the absorption spectrum, we investigate the magneto-absorption spectra of FePS_3 at different temperatures below and above $T_N \sim 120$ K. In Fig. 2(c) and (d), the magneto-absorption spectra at 80 K and 160 K are presented for $\theta = 90^\circ$ (\mathbf{E} perpendicular to the zigzag chain). It is noteworthy that the field induced-change in the absorption spectra at 80 K is similar to that observed at 4.2 K, although there is a subtle

reduction of a critical magnetic field to ~ 30 T, where the absorption is drastically enhanced. Above T_N , the effect of the magnetic field on the absorption spectra vanishes. In other words, even at 0 T, the absorption spectrum remains unsuppressed, and its shape remains almost intact up to 52 T in the magnetically ordered state. For comparison, detailed results of $\theta = 0^\circ$ are shown in Figure S1.

We calculated the LD using $\frac{|A_{90^\circ} - A_{0^\circ}|}{A_{90^\circ} + A_{0^\circ}} \times 100\%$ to directly see the change of LD in FePS_3 controlled by magnetic fields [10]. In Fig. 3(a), we show the color mapping of the LD obtained at 4.2 K. At 0 T, we observe the giant LD between 1.6 and 2.0 eV as previously reported. This LD shows almost unchanged below 40 T and suddenly drops at 40 T and eventually reaches zero around 52 T. We compare the LD at 0 and 52 T in Fig. 3(b). The maximum of LD (almost 11%) is observed at 1.75 eV, which can be controlled by a magnetic field.

To understand the drastic reduction of the dichroic signal, we first discuss the origin of the strong dichroism observed in the zero field. As shown in Fig. 3(c), in the high-spin d^6 configuration of Fe^{2+} , the one spin

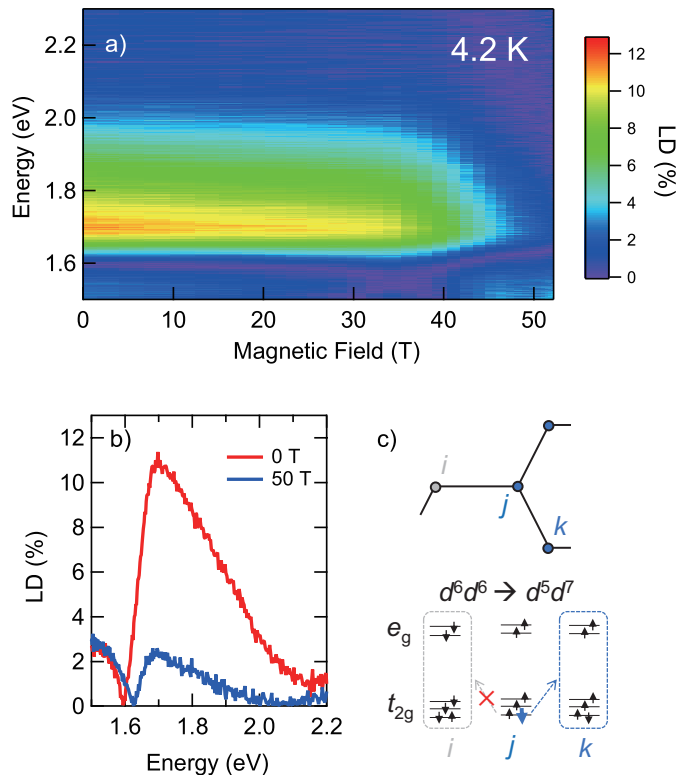


FIG. 3. a) Field dependent color mapped LD spectra up to 52 T. b) The comparison of LD spectra between 0 and 50 T. c) The schematic diagram of spin hopping in the zigzag state, that can explain the origin of the strong dichroism observed in the absent of magnetic field. The minority spins (electrons) are marked with big blue arrow.

channel is fully filled, while the other is occupied by a single electron. In the Néel antiferromagnetic state, the Pauli principle makes this electron immobile: the corresponding spin sector is fully occupied in each of the three neighboring sites. Hence, the nearest-neighbor hopping is facilitated by majority electrons, i.e. the up spin electrons at sites j and k , or the down spin electrons at site i . But in the zigzag antiferromagnetic ground state of FePS₃ the situation is very different. Here, each Fe atom has two neighbors with a parallel magnetic moment (along the zigzag chains) and one neighbor whose moment is antiparallel. Only the majority electrons can hop to the latter; by the same argument, the in-chain hopping processes are restricted to minority electrons. While both types of processes are possible, the Hund exchange gives rise to disparity: a minority electron leaves the energetically favorable high-spin state behind, while a majority electron creates the low-spin state with high energy. Thus, hopping along the chains dominates the low-energy sector of optical excitations (dipole transitions) in the zigzag state [12].

Using the same reasoning, we can expect that in the fully polarized ferromagnetic state, the low-lying optical excitations are facilitated by minority states, and dichroism is absent. However, the actual electronic structure of FePS₃ is more intricate. First, relevant hopping processes are not restricted to nearest neighbors. Hopping between the second nearest neighbor via coupling across the honeycomb voids is also present, as evidenced by the sizable magnetic exchange J_3 associated with this path. Second, for the Fe²⁺ orbital degrees of freedom are generally relevant; their fingerprint is the giant magnetic anisotropy of 22 meV/Fe measured by photoemission electron microscopy [17]. Finally, two-dimensional superlattices of FePS₃ show sizable magnetoelastic coupling [18]; structural changes at high magnetic fields can not be excluded. Hence, direct calculations of the optical conductivity in the fully polarized state are desirable for a microscopic picture.

To this end, we perform first-principles density-functional theory (DFT) calculations using the generalized gradient approximation (GGA) [19] as implemented in the full-potential code FPLO version 22 [20]. For the structural input, we use the experimental crystal structure [21] and construct two different supercells that allow for Néel-orbital [22] and zigzag magnetic order. For GGA+ U calculations, we used the Coulomb repulsion of 2.5 eV, the Hund exchange of 1 eV, and the fully localized limit as the double counting correction. This choice of interaction parameters follows [12]; other DFT+ U studies [23–26] employed similar parameters. For both cells, the Brillouin zones were uniformly sampled with approximately 2000 k -points. Optical conductivities of zigzag and ferromagnetic states were computed using the built-in optics module of FPLO. In all calculations, dipole forbidden d - d transitions are absent, because the DFT's one-

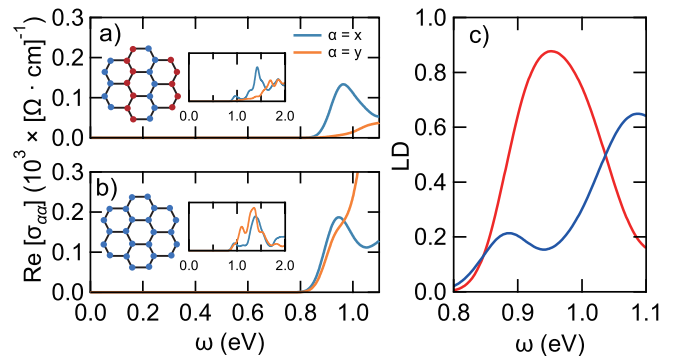


FIG. 4. Real part of optical conductivity σ in the zigzag antiferromagnetic (a) and ferromagnetic (b) states. The x axis (a axis) is parallel to the zigzag chains and the y axis (b axis) is perpendicular to both x and the normal to the magnetic plane. A Gaussian broadening of 0.05 eV is applied. Note that the absorption edge in DFT+ U calculations is controlled by the Coulomb repulsion U ; for the chosen $U = 2.5$ eV it is at ~ 0.8 eV which is significantly lower than in the experiment (~ 1.4 eV). Dichroic ratios for the zigzag antiferromagnetic (red curve) and the ferromagnetic states (blue curve) are compared in (c). Here, the dichroic ratios (LD) are obtained as $\frac{Re[\sigma_{xx}] - Re[\sigma_{yy}]}{Re[\sigma_{xx}] + Re[\sigma_{yy}]}$.

electron framework cannot describe many-body physics underlying these processes.

In Fig. 4, we compare the real part of optical conductivity $Re[\sigma_{\alpha\alpha}(\omega)]$ for the zigzag state and the ferromagnetic state. In the former case, the absorption edge for the zigzag chain direction ($\alpha = x = a$ -axis) is shifted to lower frequencies compared to the transverse direction ($\alpha = y = b$ -axis). This shift gives rise to a dichroic signal, which reaches its maximal value close to the edge, but remains sizable up to 1.5 eV. The optical conductivity of the ferromagnetic state is very different: $Re[\sigma_{yy}]$ is shifted to lower frequencies such that the absorption edge occurs at the same frequency for both directions. At the same time, $Re[\sigma_{xx}]$ does not change significantly in near the absorption edge. Both features agree with the experiment (Fig. 1). The large difference in the absolute values of dichroism can be attributed to domain structure in the samples.

For higher frequencies, the ferromagnetic state exhibits at odds with the experiment. While we cannot ultimately determine the origin of this discrepancy, a structural transition accompanying the magnetic polarization is a plausible scenario. Indeed, a strong magnetoelastic coupling is suggested from the previous high-field measurements concluded on the first order of the magnetic transition at 40 T [15]. For such effects to be accounted for in calculations, the information on the high-field crystal structure – absent so far due to technical difficulties – is needed [27]. Another possible source of discrepancies is the neglect of the spin-orbit coupling: the chosen DFT code (FPLO) does not support calculations of op-

tical spectra in the full-relativistic mode. Both of which, experimental and theoretical, are the subject of future studies.

In summary, we experimentally demonstrated that a magnetic field can switch the giant LD in the vdW anti-ferromagnet FePS₃. Below $T_N \sim 120$ K, the LD of $\sim 11\%$ is suppressed to almost zero in a wide energy range from 1.6 to 2.0 eV by a magnetic field above 40 T. The vanishing LD is associated with the change in the magnetic structure: the fully saturated state allows for a more isotropic hopping of Fe²⁺ minority electrons within the magnetic planes. This scenario is supported by DFT calculations that further hint at a first-order structural transition accompanying magnetic saturation. Recently LD has been widely used as a powerful technique to detect symmetry changes in atomically thin layers. Our study provides significant insights into the coupling between spin-order symmetry and interatomic optical transitions. The modification of spin-order symmetry by external fields is a new route to engineer multifunctional micro-devices of vdW materials.

Since FePS₃ maintains its magnetic properties even in a single monolayer, the remaining challenge is the reduction of the transition field in FePS₃. To this end, choosing an appropriate substrate that induces a moderate tensile strain in atomically thin FePS₃ is a promising route, as this alternation particularly weakens the long-range antiferromagnetic cross-hexagon exchange J_3 [24], which in turn governs the critical field.

We acknowledge Chaebin Kim for his generous assistance to the project. X.-G.Z was supported by a JSPS fellowship and funded by JSPS KAKENHI, Grant-in-Aid for JSPS Fellows No. 22F22332. A.M. was funded by JSPS KAKENHI, Fund for the Promotion of Joint International Research (Home-Returning Researcher Development Research) No. 22K21359. O.J. was supported by the Deutsche Forschungsgemeinschaft (DFG, German Research Foundation) Projects No. 247310070 and 465000489, and thanks U. Nitzsche for technical assistance. This work is also partially supported by JSPS KAKENHI, Grant-in-Aid for Transformative Research Areas (A) No.23H04859, Grant-in-Aid for Scientific Research (B) No. 18H01163, and the grant from Research Foundation for Opto-Science and Technology (Japan). The work at SNU is funded by the Leading Researcher Program of the National Research Foundation of Korea (Grant No. 2020R1A3B2079375).

[1] J. J. Sakurai and E. D. Commins, *Modern quantum mechanics*, revised edition (1995).
 [2] B. Norden, Linear and circular dichroism of polymeric pseudoisocyanine, *J. Chem. Phys.* **81**, 151 (1977).
 [3] S. Niu, G. Joe, H. Zhao, Y. Zhou, T. Orvis, H. Huyan, J. Salman, K. Mahalingam, B. Urwin, J. Wu, Y. Liu,

T. E. Tiwald, S. B. Cronin, B. M. Howe, M. Mecklenburg, R. Haiges, D. J. Singh, H. Wang, M. A. Kats, and J. Ravichandran, Giant optical anisotropy in a quasi-one-dimensional crystal, *Nat. Photonics* **12**, 392 (2018).
 [4] N. Mao, J. Tang, L. Xie, J. Wu, B. Han, J. Lin, S. Deng, W. Ji, H. Xu, K. Liu, L. Tong, and J. Zhang, Optical anisotropy of black phosphorus in the visible regime, *J. Am. Chem. Soc.* **138**, 300 (2016).
 [5] Y. Y. Wang, J. D. Zhou, J. Jiang, T. T. Yin, Z. X. Yin, Z. Liu, and Z. X. Shen, In-plane optical anisotropy in ReS₂ flakes determined by angle-resolved polarized optical contrast spectroscopy, *Nanoscale* **11**, 20199 (2019).
 [6] H. Zhang, Z. Ni, C. E. Stevens, A. Bai, F. Peiris, J. R. Hendrickson, L. Wu, and D. Jariwala, Cavity-enhanced linear dichroism in a van der waals antiferromagnet, *Nat. Photonics* **16**, 311 (2022).
 [7] C. Matthew, John, J. David, M. H. Hayrullo, H. CRS, A. Patricia, Lebre, L. Cheng, S. Suhan, H. Inho, L. Guilio, I. D. Dominik, N.-W. Paul, W. AR, S. Sidharth, S, and P. Je-Geun, Tuning dimensionality in vander-Waals antiferromagnetic Mott insulators TMPS₃, *J. Phys. Condens. Matter* **32**, 124003 (2019).
 [8] B. L. Chittari, Y. Park, D. Lee, M. Han, A. H. MacDonald, E. Hwang, and J. Jung, Electronic and magnetic properties of single-layer MPX₃ metal phosphorous trichalcogenides, *Phys. Rev. B* **94**, 184428 (2016).
 [9] K. Soonmin, K. Kangwon, K. Beom, Hyun, K. Jonghyeon, S. Kyung, Ik, L. Jae-Ung, L. Sungmin, P. Kisoo, Y. Seokhwan, K. Taehun, N. Abhishek, W. Andrew, G.-F. Mirian, L. Jiemin, C. Laurent, Z. Ke-Jin, S. Young-Woo, K. Jae, Hoon, C. Hyeonsik, and P. Je-Geun, Coherent many-body exciton in van der waals antiferromagnet NiPS₃, *Nature* **583**, 785 (2020).
 [10] Q. Zhang, K. Hwangbo, C. Wang, Q. Jiang, J.-H. Chu, H. Wen, D. Xiao, and X. Xu, Observation of giant optical linear dichroism in a zigzag antiferromagnet FePS₃, *Nano Lett.* **21**, 6938 (2021).
 [11] K. Kurosawa, S. Saito, and Y. Yamaguchi, Neutron Diffraction Study on MnPS₃ and FePS₃, *J. Phys. Soc. Jpn.* **52**, 3919 (1983).
 [12] A. Koitzsch, T. Klaproth, S. Selzer, Y. Shemerliuk, S. Aswartham, O. Janson, B. Büchner, and M. Knupfer, Intertwined electronic and magnetic structure of the van-der-Waals antiferromagnet Fe₂P₂S₆, *npj Quantum Mater.* **8**, 27 (2023).
 [13] J.-U. Lee, S. Lee, J. H. Ryoo, S. Kang, T. Y. Kim, P. Kim, C.-H. Park, J.-G. Park, and H. Cheong, Ising-type magnetic ordering in atomically thin FePS₃, *Nano Lett.* **16**, 7433 (2016).
 [14] J. Peng, X. Yang, Z. Lu, L. Huang, X. Chen, M. He, J. Shen, Y. Xing, M. Liu, Z. Qu, Z. Wang, L. Li, S. Dong, and J.-M. Liu, Ferromagnetism induced by magnetic dilution in van der waals material metal thiophosphates, *Adv. Quantum Technol.* **6**, 2200105 (2023).
 [15] A. R. Wildes, D. Lançon, M. K. Chan, F. Weickert, N. Harrison, V. Simonet, M. E. Zhitomirsky, M. V. Gvozdkova, T. Ziman, and H. M. Rønnow, High field magnetization of FePS₃, *Phys. Rev. B* **101**, 024415 (2020).
 [16] Z. Yang, X. Wang, J. Felton, Z. Kudrynskyi, M. Gen, T. Nomura, X. Wang, L. Eaves, Z. D. Kovalyuk, Y. Kohama, L. Zhang, and A. Patanè, Heavy carrier effective masses in van der Waals semiconductor Sn(SeS) revealed by high magnetic fields up to 150 T, *Phys. Rev. B* **104**,

- 085206 (2021).
- [17] L. Youjin, S. Suhan, K. Chaebin, K. Soonmin, S. Junying, K. Michel, D. Bernard, S. Tatiana, P. Sergii, N. Woongki, C. Ki-Young, K. Wondong, C. Hyeonsik, D. Peter, M., K. Armin, , and P. Je-Geun, Giant magnetic anisotropy in the atomically thin van der waals antiferromagnet feps3, *Adv. Electron. Mater.* **9**, 2200650 (2023).
- [18] S. Liu, A. Granados del Águila, D. Bhowmick, C. K. Gan, T. Thu Ha Do, M. A. Prosnikov, D. Sedmidubský, Z. Sofer, P. C. M. Christianen, P. Sengupta, and Q. Xiong, Direct Observation of Magnon-Phonon Strong Coupling in Two-Dimensional Antiferromagnet at High Magnetic Fields, *Phys. Rev. Lett.* **127**, 097401 (2021).
- [19] J. P. Perdew, K. Burke, and M. Ernzerhof, Generalized gradient approximation made simple, *Phys. Rev. Lett.* **77**, 3865 (1996).
- [20] K. Koepernik and H. Eschrig, Full-potential nonorthogonal local-orbital minimum-basis band-structure scheme, *Phys. Rev. B* **59**, 1743 (1999).
- [21] R. Brec, G. Ouvrard, A. Louisy, and J. Rouxel, *Ann. Chim.* **5**, 499 (1980), ICSD code 633080.
- [22] See Supplemental Material [URL will be inserted by publisher] for detailed plots of absorption and linear dichroism and the dependence of optical conductivity on the orbital ground state. Detailed experimental LD results obtained at different temperature are also included.
- [23] Y. Zheng, X.-x. Jiang, X.-x. Xue, J. Dai, and Y. Feng, Ab initio study of pressure-driven phase transition in FePS₃ and FePSe₃, *Phys. Rev. B* **100**, 174102 (2019).
- [24] T. Olsen, Magnetic anisotropy and exchange interactions of two-dimensional FePS₃, NiPS₃ and MnPS₃ from first principles calculations, *J. Phys. D: Appl. Phys.* **54**, 314001 (2021).
- [25] J. E. Nitschke, D. L. Esteras, M. Gutnikov, K. Schiller, S. Mañas-Valero, E. Coronado, M. Stupar, G. Zamborlini, S. Ponzoni, J. J. Baldoví, and M. Cinchetti, Valence band electronic structure of the van der Waals antiferromagnet FePS₃, *Mater. Today Electronics* **6**, 100061 (2023).
- [26] M. Amirabbasi and P. Kratzer, Orbital and magnetic ordering in single-layer FePS₃: A DFT + *U* study, *Phys. Rev. B* **107**, 024401 (2023).
- [27] A. Ikeda, Y. H. Matsuda, X. Zhou, S. Peng, Y. Ishii, T. Yajima, Y. Kubota, I. Inoue, Y. Inubushi, K. Tono, and M. Yabashi, Generating 77 T using a portable pulse magnet for single-shot quantum beam experiments, *Appl. Phys. Lett.* **120**, 142403 (2022).